

# Comparative Analysis of Metaheuristic Algorithms for Tourism Route Optimization Using Real Road Network Distances: A Case Study of Yogyakarta, Indonesia

First Author<sup>1\*</sup>, Second Author<sup>2</sup>, Third Author<sup>2</sup> <sup>1</sup>Department, University, City, Indonesia  
 email@university.ac.id <sup>2</sup>Department, University, City, Indonesia \*Corresponding author

**Abstract**—This study evaluates four metaheuristic algorithms for tourism route optimization in Yogyakarta Special Region, Indonesia, formulated as a Travelling Salesman Problem over 25 tourist attractions. Road distances were computed via Dijkstra's algorithm on an OpenStreetMap network of 153,334 nodes and 200,104 edges. Simulated Annealing (SA) with 2-opt produced the shortest mean route of 283.82 km ( $\sigma = 0.08$  km), followed by Max-Min Ant System (MMAS, 284.35 km), Ant Colony System (ACS, 285.49 km), and Genetic Algorithm (GA, 302.13 km). All pairwise differences were significant by Wilcoxon signed-rank tests ( $p < 0.05$ ). ACS was 10.7 times faster than SA. Parameter sensitivity analysis of 27 MMAS configurations revealed strong interactions between the pheromone weight  $\alpha$  and evaporation rate  $\rho$ . A mean road-to-Euclidean ratio of 1.18 confirms that real road data is necessary for practical route planning.

**Index Terms**—tourism route optimization, Travelling Salesman Problem, Ant Colony Optimization, Simulated Annealing, Genetic Algorithm, OpenStreetMap, Yogyakarta

## I. INTRODUCTION

YOGYAKARTA Special Region (Daerah Istimewa Yogyakarta, DIY) receives more than 4.5 million visitors annually, offering attractions from the UNESCO-listed Borobudur and Prambanan temples to coastal and volcanic landscapes [1]. Visitors wanting to cover many sites in limited time face a route-planning problem that maps onto the Travelling Salesman Problem (TSP), which is NP-hard and grows factorially with the number of locations [2], [3].

Metaheuristic algorithms provide approximate solutions within practical time budgets. Ant Colony Optimization (ACO) variants exploit pheromone-based reinforcement [4], [5], Genetic Algorithms (GA) use selection, crossover, and mutation [6], and Simulated Annealing (SA) escapes local optima through a cooling schedule [7]. Their relative performance depends on problem size, distance metric, and parameter settings [2], [3].

A persistent shortcoming in tourism route studies is the reliance on Euclidean or haversine distances [8]. Road networks contain one-way streets, bridges, and topographic detours causing actual distances to exceed straight-line estimates by 15–20%. Yogyakarta's volcanic-slope-to-coast geography amplifies these discrepancies.

This paper addresses this gap by computing a  $25 \times 25$  road-distance matrix via Dijkstra's algorithm on the OpenStreetMap network for DIY (153,334 nodes, 200,104 edges)

and comparing Max-Min Ant System (MMAS), Ant Colony System (ACS), GA, and SA over 30 independent runs. The comparison covers solution quality, variance, computation time, convergence behaviour, and statistical significance. Parameter sensitivity and scalability analyses complement the main experiment.

The contributions of this study are threefold. First, we provide the first multi-algorithm metaheuristic comparison for tourism routing in Yogyakarta that uses real road network distances rather than Euclidean approximations. Second, we quantify the road-to-Euclidean distance deviation across 300 attraction pairs, providing empirical evidence for why straight-line distances are inadequate for practical route planning in this region. Third, we present a parameter sensitivity analysis of MMAS that reveals the interaction structure among its three main control parameters, offering guidance for practitioners tuning ACO algorithms on similar problem instances.

## II. RELATED WORK

### A. TSP and Metaheuristics

The TSP seeks the minimum-cost Hamiltonian cycle through  $n$  cities; for symmetric TSP the solution space contains  $(n - 1)!/2$  tours [2]. Advanced heuristics such as LKH [9] produce near-optimal solutions for large instances, but population-based and trajectory-based metaheuristics remain the practical choice for resource-constrained settings [10].

Dorigo et al. [4] introduced Ant System; Stützle and Hoos [5] proposed MMAS with bounded pheromone trails; Dorigo and Gambardella [11] developed ACS with pseudo-random selection and local pheromone decay. Recent ACO work includes adaptive heuristics [12], large-scale strategies [13], and hybrid methods [14], [15]. GA for TSP uses permutation-preserving operators such as OX crossover [6], [16], sometimes combined with reinforcement learning [17]. SA with 2-opt [7], [18] remains competitive for moderate instances [19].

### B. Tourism Route Optimization

Ruiz-Meza and Montoya-Torres [20] surveyed tourist trip design, covering orienteering formulations with time windows [21], [22]. Sun et al. [23] proposed multi-objective ACO for route recommendation, incorporating travel time and tourist preferences alongside distance. Most studies in tourism

routing use Euclidean or haversine distances for simplicity, but this assumption has been questioned by vehicle routing researchers. OSMnx [24], [25] has made real road network extraction practical for any region worldwide, and Boyaci et al. [8] showed that Euclidean approximations introduce 10–30% errors in European vehicle routing. Tatit et al. [26] confirmed similar deviations for spatial database queries, noting that the error varies with road network density and terrain.

Within Indonesia, Nasution et al. [27] applied vehicle routing with time windows to tourism itineraries but relied on Google Maps API calls rather than a pre-computed road network. Fathurrohman et al. [28] formulated a green orienteering problem for Yogyakarta that considered carbon emissions [29], but tested only a single algorithm. Neither study provided the multi-algorithm statistical comparison over pre-computed real road distances offered here, nor did they analyse parameter sensitivity or scalability behaviour.

### III. MATERIALS AND METHOD

#### A. Problem Formulation

Let  $V = \{1, 2, \dots, n\}$  be  $n = 25$  tourist attractions. The objective is to find a permutation  $\pi$  minimising:

$$D(\pi) = \sum_{i=1}^{n-1} d(\pi_i, \pi_{i+1}) + d(\pi_n, \pi_1) \quad (1)$$

where  $d(i, j)$  is the shortest road distance between attractions  $i$  and  $j$ .

#### B. Study Area and Data

Twenty-five attractions in DIY were selected across six categories: cultural heritage sites (Kraton, Taman Sari, Kotagede), historical landmarks (Benteng Vredeburg, Tugu), religious temples (Borobudur, Prambanan, Ratu Boko), nature and recreation areas (Parangtritis, Indrayanti, Goa Pindul, Hutan Pinus Mangunan, Tebing Breksi, HeHa Sky View), museums (Sonobudoyo, Affandi, Ullen Sentalu), and urban attractions (Malioboro, Beringharjo, Taman Pintar, Gembira Loka Zoo, Purawisata, Monumen Jogja Kembali, Alun-Alun Utara, Alun-Alun Kidul). Table I lists each attraction with its geographic coordinates.

The road network was downloaded via OSMnx [24] using the query “Daerah Istimewa Yogyakarta, Indonesia” with `network_type=drive`, yielding 153,334 nodes and 200,104 edges after undirected conversion. Each attraction was snapped to its nearest network node, and the  $25 \times 25$  distance matrix was computed using Dijkstra’s algorithm. Fig. 1 shows the spatial distribution of these attractions. The study area spans roughly 60 km north-to-south (from Borobudur/Ullen Sentalu in the highlands to Pantai Indrayanti on the coast) and 50 km east-to-west (from Goa Pindul to Borobudur), with a dense cluster of 10 attractions within the urban core of Yogyakarta city.

The resulting distance matrix is visualised in Fig. 2. The largest pairwise distance is 93.3 km (Borobudur to Pantai Indrayanti), while the smallest is 0.3 km (Alun-Alun Utara to Museum Sonobudoyo). Urban core attractions form a visible

low-distance block in the upper-left portion of the matrix. The asymmetry between some pairs reflects the one-way street structure retained during Dijkstra computation before the matrix was symmetrised by taking the minimum of each directed pair.

TABLE I  
TOURIST ATTRACTIONS IN YOGYAKARTA SPECIAL REGION ( $n = 25$ ).

ID	Name	Lat.	Long.
1	Kraton Yogyakarta	-7.805	110.364
2	Taman Sari Water Castle	-7.810	110.359
3	Benteng Vredeburg Museum	-7.800	110.366
4	Tugu Yogyakarta	-7.783	110.367
5	Malioboro Street	-7.793	110.366
6	Pasar Beringharjo	-7.798	110.366
7	Museum Sonobudoyo	-7.802	110.364
8	Alun-Alun Kidul	-7.812	110.364
9	Alun-Alun Utara	-7.803	110.364
10	Taman Pintar Science Park	-7.801	110.367
11	Gembira Loka Zoo	-7.806	110.395
12	Museum Affandi	-7.783	110.397
13	Kotagede Heritage Area	-7.827	110.398
14	Monumen Jogja Kembali	-7.750	110.377
15	Purawisata	-7.801	110.374
16	Candi Prambanan	-7.752	110.491
17	Candi Ratu Boko	-7.770	110.489
18	Tebing Breksi	-7.762	110.504
19	Museum Ullen Sentalu	-7.604	110.426
20	Candi Borobudur	-7.608	110.204
21	Pantai Parangtritis	-8.025	110.326
22	Hutan Pinus Mangunan	-7.931	110.431
23	Goa Pindul	-7.953	110.650
24	Pantai Indrayanti	-8.150	110.613
25	HeHa Sky View	-7.855	110.454

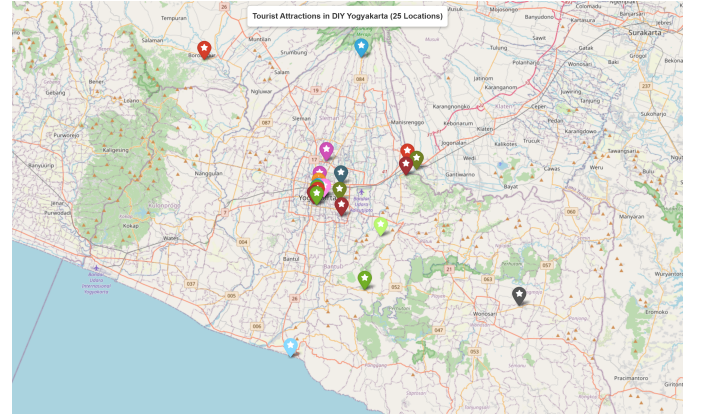


Fig. 1. Spatial distribution of 25 tourist attractions in Yogyakarta Special Region.

#### C. Algorithm Implementations

All algorithms were implemented in Python with NumPy vectorisation. The core mechanisms are formalised below.

**ACO transition rule.** Both MMAS and ACS construct tours by having  $m = 25$  ants choose the next city probabilistically. For ant  $k$  at city  $i$ , the probability of moving to unvisited city  $j$  is:

$$p_{ij}^k = \frac{[\tau_{ij}]^\alpha [\eta_{ij}]^\beta}{\sum_{l \in \mathcal{N}_i^k} [\tau_{il}]^\alpha [\eta_{il}]^\beta}, \quad j \in \mathcal{N}_i^k \quad (2)$$

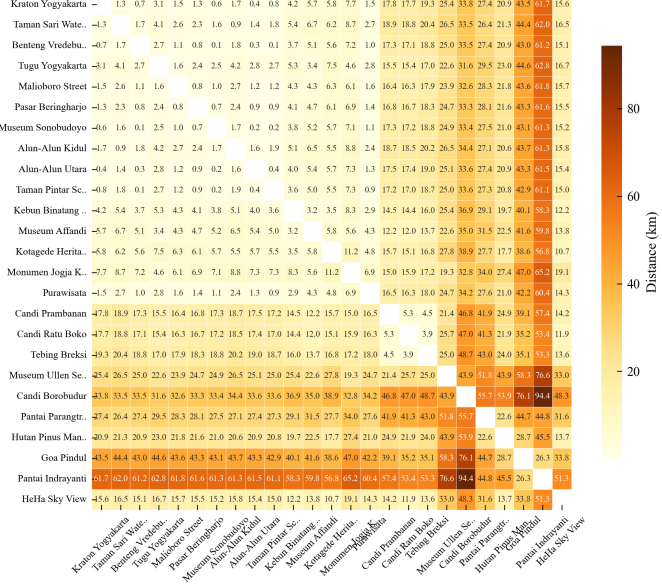


Fig. 2. Road distance matrix (km) for the 25 tourist attractions. Darker cells indicate longer distances. The urban core attractions (IDs 1–10) form a low-distance cluster in the upper-left block.

where  $\tau_{ij}$  is the pheromone on edge  $(i, j)$ ,  $\eta_{ij} = 1/d(i, j)$  is the heuristic desirability,  $\mathcal{N}_i^k$  is the set of unvisited cities, and  $\alpha$ ,  $\beta$  control the relative influence of pheromone versus distance.

**MMAS** [5] restricts pheromone trails to  $[\tau_{\min}, \tau_{\max}]$ . After each iteration, only the best ant deposits pheromone:

$$\tau_{ij} \leftarrow \text{clamp}[(1 - \rho) \tau_{ij} + \Delta \tau_{ij}^{\text{best}}, \tau_{\min}, \tau_{\max}] \quad (3)$$

where  $\Delta \tau_{ij}^{\text{best}} = 1/D^{\text{best}}$  if edge  $(i, j)$  belongs to the best tour. Bounds are set as  $\tau_{\max} = 1/(\rho \cdot D_{\text{NN}})$  and  $\tau_{\min} = \tau_{\max}/(2n)$ . Parameters:  $\alpha = 1.0$ ,  $\beta = 3.0$ ,  $\rho = 0.02$ , 500 iterations, stagnation re-initialisation after 100 iterations without improvement.

**ACS** [11] uses a pseudo-random proportional rule: with probability  $q_0$  the ant greedily selects  $\arg \max_j [\tau_{ij}]^\alpha [\eta_{ij}]^\beta$ ; otherwise it samples from Eq. (2). After each step, local pheromone decay is applied:  $\tau_{ij} \leftarrow (1 - \xi) \tau_{ij} + \xi \tau_0$ , with  $\tau_0 = 1/(n \cdot D_{\text{NN}})$ . Parameters:  $q_0 = 0.9$ ,  $\xi = 0.1$ ,  $\rho = 0.1$ , 500 iterations.

**GA** used Order Crossover (OX) on permutation chromosomes with population 100, crossover rate 0.8, swap mutation rate 0.02, tournament selection ( $k = 3$ ), 10% elitism, 500 generations with early stopping after 100 generations without improvement.

**SA** explores the neighbourhood by 2-opt moves. At temperature  $T$ , a candidate solution with cost difference  $\Delta D = D' - D$  is accepted with probability:

$$P(\text{accept}) = \begin{cases} 1 & \text{if } \Delta D < 0 \\ \exp(-\Delta D/T) & \text{otherwise} \end{cases} \quad (4)$$

A 2-opt move reverses a subtour segment between positions  $i$

and  $j$ . The cost change is evaluated in  $O(1)$ :

$$\begin{aligned} \Delta D &= d(\pi_i, \pi_j) + d(\pi_{i+1}, \pi_{j+1}) \\ &\quad - d(\pi_i, \pi_{i+1}) - d(\pi_j, \pi_{j+1}) \end{aligned} \quad (5)$$

Parameters:  $T_0 = 10,000$ , cooling rate  $\gamma = 0.999$ ,  $T_{\text{end}} = 1.0$ , 50 iterations per temperature step ( $\sim 9,200$  total steps).

**Nearest Neighbour (NN)** baseline was executed from all 25 starting nodes; the shortest tour was reported.

## D. Experimental Design

Each stochastic algorithm was executed 30 times with seeds 42–71. The experimental programme consisted of four parts: (1) main comparison, with 120 stochastic runs (30 per algorithm) plus one deterministic NN run; (2) parameter sensitivity, testing 27 MMAS configurations by combining three levels each of pheromone weight (0.5, 1.0, 2.0), heuristic weight (2, 3, 5), and evaporation rate (0.02, 0.05, 0.10), with 10 runs per configuration; (3) scalability analysis on subsets of 10, 12, 15, and 20 attractions, 10 runs each; and (4) Wilcoxon signed-rank tests at a 0.05 significance level for all six pairwise algorithm comparisons.

**Performance metrics.** Algorithm quality is measured by the Relative Percentage Deviation (RPD) from the best-known solution  $D^*$ :

$$\text{RPD} = \frac{D - D^*}{D^*} \times 100\% \quad (6)$$

Solution consistency is assessed by the Coefficient of Variation (CV), defined as the standard deviation divided by the mean distance. Computational efficiency is reported as mean wall-clock time per run.

## IV. RESULTS AND DISCUSSION

### A. Algorithm Performance

Table II summarises all 30 independent runs per algorithm. SA and MMAS both discovered the same best-known tour of 283.76 km, but SA was far more consistent, with a mean only 0.06 km above the best and a standard deviation of just 0.08 km. SA's RPD of 0.02% and CV of 0.03% stand in sharp contrast to GA's 6.47% RPD and 2.25% CV, reflecting the difference between a tightly focused local search and a population-based method that struggles with permutation structure. ACS offers a practical middle ground: its tours averaged about 1.7 km longer than SA's, but it ran 10.7 times faster (0.327 s versus 3.496 s). GA performed worst overall, with a mean tour length that exceeded even the deterministic NN baseline, confirming that basic OX crossover alone cannot solve this 25-node problem effectively.

Fig. 3 provides a visual comparison of the key metrics from Table II. The distance panel makes the gap between GA and the other algorithms immediately apparent, while the time panel shows that ACS and GA are the fastest algorithms but for very different reasons: ACS finishes quickly because its pseudo-random rule concentrates search effort, while GA's population-based evaluation is inherently parallel.

The run-level distributions in Fig. 4 reveal how each algorithm explores the solution space. SA found the global

TABLE II  
ALGORITHM PERFORMANCE OVER 30 RUNS. BEST VALUES IN BOLD; NN IS DETERMINISTIC. RPD FROM  $D^* = 283.76$  km.

	Best (km)	Mean (km)	Std (km)	RPD (%)	Time (s)
MMAS	283.76	284.35	0.85	0.21	1.704
ACS	283.94	285.49	1.80	0.61	<b>0.327</b>
GA	291.31	302.13	6.79	6.47	0.676
SA	<b>283.76</b>	<b>283.82</b>	<b>0.08</b>	<b>0.02</b>	3.496
NN	297.10	297.10	0.00	4.70	0.001

optimum in 19 of 30 runs; the remaining 11 settled on one of three near-optimal tours within 0.21 km of the best, showing that the 2-opt neighbourhood funnels solutions toward a small family of structurally similar tours. MMAS hit the optimum only once, but 19 runs still fell within 0.06% of it, forming a tight cluster. ACS shows a distinct bimodal pattern: about half the runs reached its best tour, while the other half got trapped on longer routes because the high exploitation probability (0.9) can lock the colony onto early pheromone trails. GA produced the widest spread (26.7 km between best and worst), with no concentration around any single tour structure.

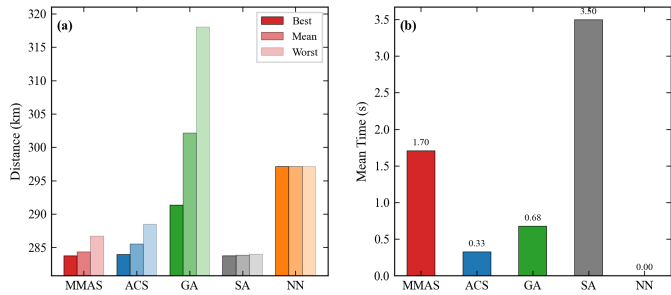


Fig. 3. Summary of algorithm performance. Left: best, mean, and worst distances; right: mean computation time per run.

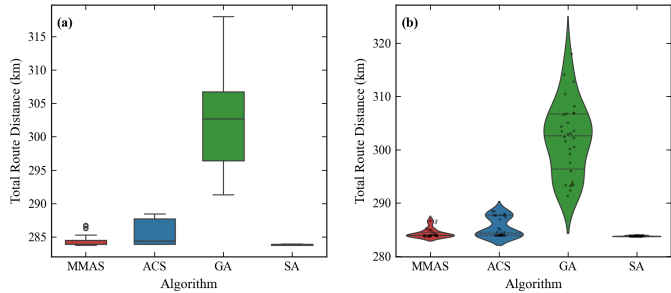


Fig. 4. Distribution of best distances across 30 runs. Box plots show median, interquartile range, and outliers; violin overlays show kernel density.

Table III reports the Wilcoxon signed-rank test results for all six pairwise comparisons. Every pair is statistically significant ( $p < 0.05$ ), establishing the ranking SA > MMAS > ACS > GA. Even the closest pair, MMAS versus ACS, yielded  $p = 0.011$ , while the remaining five returned  $p < 0.0001$ . For every pair involving GA, all 30 matched observations favoured the competing algorithm ( $W = 0$ ).

TABLE III  
WILCOXON SIGNED-RANK TEST RESULTS (SIGNIFICANCE LEVEL 0.05). ALL SIX PAIRWISE COMPARISONS ARE SIGNIFICANT.

Pair	$W$	$p$ -value
MMAS vs ACS	68.0	0.011
MMAS vs GA	0.0	< 0.0001
MMAS vs SA	31.0	< 0.0001
ACS vs GA	0.0	< 0.0001
ACS vs SA	9.0	< 0.0001
GA vs SA	0.0	< 0.0001

### B. Convergence Behaviour

Fig. 5 plots the mean best-so-far distance over 500 iterations, averaged across 30 runs. The four algorithms converge at very different rates.

SA starts with the poorest initial solutions (random permutations), but descends the fastest and reaches its final value by roughly iteration 223, less than half the allocated budget. The 2-opt neighbourhood produces large improving moves early on, and the Metropolis criterion (Eq. 4) keeps enough randomness to escape local optima before the temperature drops too low.

MMAS follows a steadier trajectory. Its bounded pheromone trails prevent premature convergence, so the colony keeps improving until around iteration 357. The trade-off is slower final refinement compared to SA, but no run stagnated early.

ACS shows the fastest initial descent among the ACO variants, cutting over 15 km in the first 50 iterations. It then plateaus around iteration 178, much sooner than MMAS. The high exploitation probability (0.9) drives aggressive early search but leaves too little diversity for later refinement.

GA converged the most slowly. Its initial solutions were substantially longer because it starts from purely random permutations without a nearest-neighbour seed. GA was still improving at iteration 500, suggesting the budget was insufficient and that hybridisation with local search operators could narrow the gap. The convergence profiles explain why the standard deviations in Table II differ so widely: SA's early convergence leaves little room for run-to-run variation, while GA's incomplete convergence means each run may stop at a different point along its descent curve. MMAS and ACS fall in between, with MMAS achieving lower variance thanks to its longer convergence window.

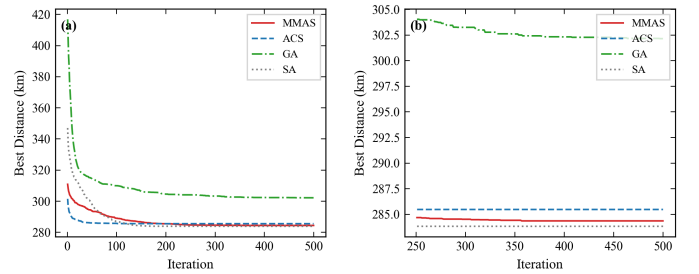


Fig. 5. Convergence curves showing mean best-so-far distance over iterations (averaged across 30 runs). SA converges fastest to the lowest value; GA is still improving at iteration 500.

### C. Optimised Routes

Fig. 6 compares the best routes found by each algorithm. The optimal tour (283.76 km, found by both SA and MMAS) traces a loop that avoids crossing legs. Starting from the urban core (Kraton, Taman Sari, Alun-Alun Kidul), the route heads southeast through Purawisata and Gembira Loka Zoo to Kotagede, then swings south to the coast (Parangtritis, Indrayanti, Goa Pindul). From there it climbs northeast through the hills (Hutan Pinus Mangunan, HeHa Sky View) to the eastern temples (Ratu Boko, Tebing Breksi, Prambanan), north to Ullen Sentalu, west to Borobudur, and back through northern Yogyakarta (Monumen Jogja Kembali, Museum Affandi, Tugu, Malioboro) to close the loop. This geographic clustering minimises backtracking across the region's distinct tourism zones.

The ACS route followed a nearly identical sequence, differing by only one swap in the urban core and adding less than 0.2 km. GA's best tour contained visible detours where the route jumped between non-adjacent zones instead of completing one cluster before moving to the next. This is a typical weakness of OX crossover, which preserves relative ordering but does not directly optimise edge connections.



Fig. 6. Best routes found by each algorithm on the road network. SA and MMAS share the same optimal tour structure (283.76 km); ACS differs by one swap (283.94 km); GA shows visible detours (291.31 km).

### D. Parameter Sensitivity

Fig. 7 shows how MMAS performance varies across 27 configurations (10 runs each), combining three levels each of pheromone weight, heuristic weight, and evaporation rate. The best configuration (pheromone weight 2.0, heuristic weight 2, evaporation rate 0.02) achieved a mean distance of 283.82 km, matching SA in Table II, while the worst reached 290.22 km, a 6.4 km gap from parameter choice alone.

The interaction between pheromone weight and evaporation rate dominated. When pheromone weight is high, low evaporation works best because the colony can steadily reinforce good edges over many iterations. When pheromone weight is low, the trails carry less information and need faster refreshing; higher evaporation compensates by clearing

outdated pheromone and encouraging re-exploration. At the lowest pheromone weight, raising the evaporation rate from 0.02 to 0.10 reduced the mean distance by 2.3 km.

The heuristic weight had a smaller effect. Changing it from 2 to 5 within any panel rarely shifted the mean distance by more than 1 km. One exception occurred at moderate pheromone weight with high heuristic weight and mid-range evaporation, where all 10 runs converged to the same tour with zero variance, a sign that a strong distance heuristic can force complete convergence at the cost of solution diversity.

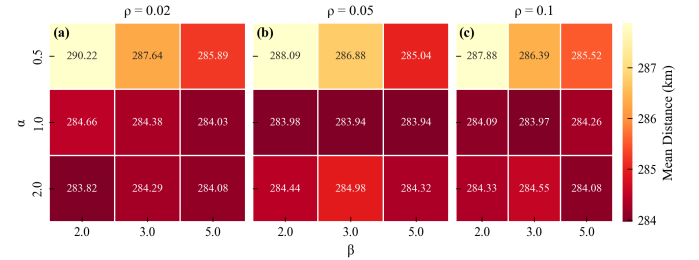


Fig. 7. MMAS parameter sensitivity heatmaps. Each cell shows the mean distance (km) over 10 runs. The best configuration (pheromone weight 2.0, heuristic weight 2, evaporation rate 0.02) matches SA's mean of 283.82 km.

### E. Scalability

Fig. 8 reports mean distance and computation time for subsets of 10, 12, 15, and 20 attractions (10 runs each), alongside the full 25-attraction results from Table II. At 12 or fewer attractions, all four metaheuristics found the optimal tour in every run, though GA already showed non-zero variance at 12 attractions.

The algorithms separated at 15 attractions. MMAS, ACS, and SA still found the optimum reliably, but GA's mean rose to 3.1% above the best-known solution. At 20 attractions, SA still produced near-perfect results, MMAS and ACS stayed within 0.2%, but GA's gap grew to 5.2%. This widening continued at 25 attractions, where GA trailed by 6.5% (Table II).

The bottom panel of Fig. 8 shows runtime. MMAS and ACS grew roughly quadratically with problem size, consistent with the  $O(m \cdot n^2)$  cost of their pheromone update mechanism, where  $m = n$  ants each evaluate  $n$  candidate cities at each step. GA scaled linearly because its population size and number of generations were held constant. SA's runtime stayed nearly constant at about 3.5 s regardless of problem size, since the number of temperature steps is fixed by the cooling schedule, and each 2-opt evaluation is  $O(1)$  using the incremental cost formula in Eq. 5. This constant-time property makes SA attractive for larger tourism networks where computation budget is limited, though the quality advantage may diminish as problem size grows beyond the 25-node range tested here.

### F. Euclidean Versus Road Distance

Euclidean distances are an imperfect proxy for actual travel. To quantify the gap, we computed the detour ratio for each attraction pair:

$$r_{ij} = \frac{d_{\text{road}}(i, j)}{d_{\text{euclid}}(i, j)} \quad (7)$$

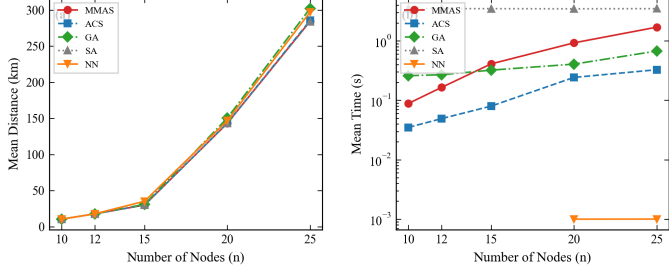


Fig. 8. Scalability analysis for 10, 12, 15, 20, and 25 attractions. Top: mean distance; bottom: mean computation time. GA diverges as problem size increases; SA runtime remains constant.

where a ratio of 1 would mean a perfectly straight road.

Fig. 9 compares the two distance measures across all 300 attraction pairs. The scatter plot shows a strong linear correlation ( $R^2 = 0.97$ ), but with a consistent positive bias: road distances averaged 18% longer (mean ratio 1.18, standard deviation 0.12). The ratio was lowest (around 1.05) for pairs connected by direct highway segments, such as the Yogyakarta–Prambanan corridor along the main east-west highway. The highest ratios (up to 1.72) occurred for pairs separated by rivers, volcanic slopes, or dense urban fabric where roads must follow indirect paths. For example, the Euclidean distance from Candi Borobudur to Pantai Indrayanti is 48 km, but the road distance is 83 km because vehicles must descend the Menoreh hills, cross through the Yogyakarta urban area, and navigate the winding Gunung Kidul karst roads to reach the coast.

Because the bias is consistent, the errors compound across a multi-stop tour. For the 25-attraction problem, relying on Euclidean distances would underestimate total tour length by roughly 40–50 km, enough to make a planned day trip infeasible. More critically, Euclidean-based optimization may produce a different tour order than road-based optimization, because the relative ranking of edge costs changes when detour ratios vary across the network. Two attractions that appear close in Euclidean space may be far apart on the road network if a river or mountain range lies between them.

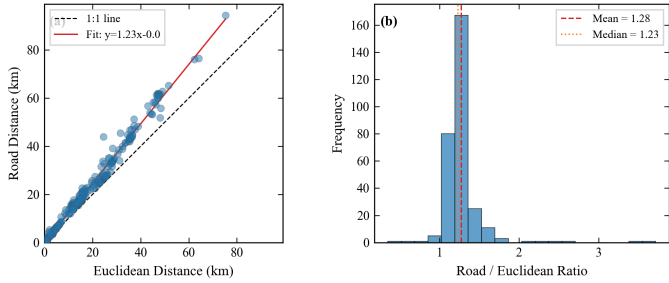


Fig. 9. Euclidean versus road distance comparison. Left: scatter plot with linear regression ( $R^2 = 0.97$ ); right: histogram of detour ratios (mean 1.18, range 1.05–1.72).

## G. Discussion

**Algorithm selection trade-offs.** SA with 2-opt is the best choice when a few seconds of computation is acceptable,

such as offline trip planning tools or pre-computed itinerary brochures. ACS suits interactive applications better, for example a mobile app recalculating routes in real time, because it runs an order of magnitude faster while producing tours only marginally longer (Table II). MMAS falls between the two: more reliable than ACS ( $p = 0.011$ , Table III), but slower. GA with basic OX crossover is not competitive at this problem size (Fig. 8), though hybridising it with local search [17] or edge-assembly crossover [6] would likely help.

**Why SA outperforms ACO on this instance.** The 25-attraction problem has a particular structure that favours SA with 2-opt. Most of the attractions cluster geographically into four or five groups (the urban core, the eastern temples, the southern coast, the highlands, and Borobudur). A 2-opt move can efficiently remove crossing edges between these clusters, producing large distance improvements in a single step. ACO variants, by contrast, build tours node by node and rely on pheromone accumulation over many iterations to discover the same cluster structure. For this moderate problem size, the direct edge-swap mechanism of 2-opt converges faster than pheromone-guided construction. On larger or less clustered instances, the balance might shift in favour of ACO, which can explore a wider set of tour structures through its population of ants.

**Practical implications.** The optimal 283.76 km tour reported in Table II translates to roughly 7 hours of driving at Yogyakarta's typical mixed-road speed of 40 km/h. Combined with 30–60 minutes spent at each attraction, visiting all 25 sites listed in Table I would span 3–4 days. The geographic clustering visible in the optimal route (Fig. 6) suggests a natural breakdown into daily itineraries: (1) the urban core (Kraton, Malioboro, Taman Sari, and surrounding sites), (2) the eastern temple complex (Prambanan, Ratu Boko, Tebing Breksi) combined with the northern highland (Ullen Sentalu), (3) the southern coast (Parangtritis, Indrayanti, Goa Pindul, Hutan Pinus), and (4) a western excursion to Borobudur. Tour operators could use these clusters as ready-made day-trip modules.

Looking at the distance matrix in Fig. 2, the urban core attractions (IDs 1–10) are all within 5 km of each other, making them walkable or reachable by short rides. The coastal attractions (Parangtritis, Indrayanti) are 30–50 km from the urban core, and Goa Pindul is another 40 km east, so the southern loop alone requires substantial driving. Borobudur sits 40 km northwest and is best combined with Ullen Sentalu (25 km northeast of Borobudur) as a full-day excursion from the city.

**Comparison with related work.** The 18% road-to-Euclidean deviation matches findings by Boyaci et al. [8] for European vehicle routing and Tatit et al. [26] for spatial query accuracy, indicating that this bias is not specific to Yogyakarta. Unlike Sun et al. [23] and Nasution et al. [27], who used simplified distance metrics, our results show that real road distances alter both absolute tour lengths and the relative ranking of near-optimal solutions. The parameter sensitivity results also align with the tuning guidance of Kaushik and Nadeem [30], who noted that ACO parameters interact and should not be tuned in isolation.

**Limitations.** This study optimises total distance only. Travellers also care about travel time, entrance fees, opening hours, and personal preferences; multi-objective formulations [20], [23] would address these. The road distances are static and do not account for traffic congestion or time-of-day variations, which can be substantial in Yogyakarta: the Malioboro corridor and the road to Borobudur experience heavy congestion during holidays and weekends. The analysis covers a single destination with 25 attractions; testing on larger instances (50–100 attractions) or other Indonesian cities with different road topologies would test generalisability. The comparison also does not include orienteering formulations with time windows [22], [28], which would be more realistic for tourists with limited time, or near-exact solvers such as LKH [9], which would provide a tighter upper bound on solution quality.

## V. CONCLUSION

This study compared four metaheuristic algorithms (MMAS, ACS, GA, and SA) for a 25-attraction tourism route optimisation problem in Yogyakarta, formulated as a TSP over real road distances extracted from OpenStreetMap. Three principal findings emerged. First, SA with 2-opt consistently produced the shortest and most reliable tours, achieving a mean of 283.82 km across 30 runs with a standard deviation below 0.1 km. All pairwise differences were statistically significant ( $p < 0.05$ ), yielding a clear ranking of SA, MMAS, ACS, and GA from best to worst. Second, ACS offered the best speed-quality trade-off, completing runs an order of magnitude faster than SA while producing tours only marginally longer, making it suitable for real-time applications. Third, the mean road-to-Euclidean detour ratio of 1.18 confirms that Euclidean distances systematically underestimate travel costs, reinforcing the need for real road network data in tourism route planning.

Parameter sensitivity analysis revealed that MMAS performance varies by up to 6.4 km depending on parameter settings, with a strong interaction between the pheromone weight and evaporation rate. Scalability tests showed that GA's quality gap widens with problem size, while the other three algorithms remain robust up to 25 attractions.

Future work should extend this framework in several directions. Multi-objective formulations that include travel time, entrance fees, opening hours, and visitor preferences would produce more practical itineraries. Incorporating dynamic traffic data from sources such as Google Maps or local traffic monitoring systems would improve the accuracy of travel time estimates, particularly during peak tourist seasons when congestion around Borobudur and Malioboro can double travel times. Testing the approach on other Indonesian tourism destinations, such as Bali, Bandung, or Lombok, would help assess generalisability across different road network topologies and attraction distributions.

## DECLARATION OF COMPETING INTEREST

The authors declare no known competing financial interests or personal relationships that could have influenced this work.

## DATA AVAILABILITY

The source code, distance matrices, and experimental results are available at [repository URL].

## REFERENCES

- [1] Badan Pusat Statistik DIY, "Statistik kepariwisataan daerah istimewa yogyakarta," BPS Provinsi D.I. Yogyakarta, Tech. Rep., 2023.
- [2] B. Toaza and D. Esztergar-Kiss, "A review of metaheuristic algorithms for solving TSP-based scheduling optimization problems," *Applied Soft Computing*, vol. 148, p. 110908, 2023.
- [3] K. Rajwar, K. Deep, and S. Das, "An exhaustive review of the metaheuristic algorithms for search and optimization: taxonomy, applications, and open challenges," *Artificial Intelligence Review*, vol. 56, no. 11, pp. 13 187–13 257, 2023.
- [4] M. Dorigo, V. Maniezzo, and A. Colorni, "Ant system: optimization by a colony of cooperating agents," *IEEE Transactions on Systems, Man, and Cybernetics, Part B (Cybernetics)*, vol. 26, no. 1, pp. 29–41, 1996.
- [5] T. Stützle and H. H. Hoos, "MAX-MIN ant system," *Future Generation Computer Systems*, vol. 16, no. 8, pp. 889–914, 2000.
- [6] Y. Deng, J. Xiong, and Q. Wang, "A hybrid cellular genetic algorithm for the traveling salesmen problem," *Mathematical Problems in Engineering*, vol. 2021, p. 6697598, 2021.
- [7] S. Kirkpatrick, C. D. Gelatt, and M. P. Vecchi, "Optimization by simulated annealing," *Science*, vol. 220, no. 4598, pp. 671–680, 1983.
- [8] B. Boyaci, T. H. Dang, and A. N. Letchford, "Vehicle routing on road networks: how good is Euclidean approximation?" *Computers & Operations Research*, vol. 129, p. 105197, 2021.
- [9] J. Zheng, K. He, J. Zhou, Y. Jin, and C.-M. Li, "Reinforced Lin-Kernighan-Helsgaun algorithms for the traveling salesman problems," *Knowledge-Based Systems*, vol. 260, p. 110144, 2023.
- [10] M. Yousefikhoshbakht, "Solving the traveling salesman problem: a modified metaheuristic algorithm," *Complexity*, vol. 2021, p. 6668345, 2021.
- [11] M. Dorigo and L. M. Gambardella, "Ant colony system: a cooperative learning approach to the traveling salesman problem," *IEEE Transactions on Evolutionary Computation*, vol. 1, no. 1, pp. 53–66, 1997.
- [12] P. Du, N. Liu, H. Zhang, and J. Lu, "An improved ant colony optimization based on an adaptive heuristic factor for the traveling salesman problem," *Journal of Advanced Transportation*, vol. 2021, p. 6642009, 2021.
- [13] R. Skinderowicz, "Improving ant colony optimization efficiency for solving large TSP instances," *Applied Soft Computing*, vol. 120, p. 108653, 2022.
- [14] T. Fei, X. Wu, L. Zhang, Y. Zhang, and L. Chen, "Research on improved ant colony optimization for traveling salesman problem," *Mathematical Biosciences and Engineering*, vol. 19, no. 8, pp. 8152–8186, 2022.
- [15] T. Hao, Y. Wu, J. Zhang, and J. Zhang, "Study on a hybrid algorithm combining enhanced ant colony optimization and double improved simulated annealing via clustering in the TSP," *PeerJ Computer Science*, vol. 9, p. e1609, 2023.
- [16] S. Cao, "An optimal round-trip route planning method for tourism based on improved genetic algorithm," *Computational Intelligence and Neuroscience*, vol. 2022, p. 7665874, 2022.
- [17] Y. Ruan, W. Cai, and J. Wang, "Combining reinforcement learning algorithm and genetic algorithm to solve the traveling salesman problem," *Journal of Engineering*, vol. 2024, no. 6, p. e12393, 2024.
- [18] G. A. Croes, "A method for solving traveling-salesman problems," *Operations Research*, vol. 6, no. 6, pp. 791–812, 1958.
- [19] P. H. Gunawan and Iryanto, "Simulated annealing – 2 opt algorithm for solving traveling salesman problem," *International Journal of Computing*, vol. 22, no. 1, pp. 43–50, 2023.
- [20] J. Ruiz-Meza and J. R. Montoya-Torres, "A systematic literature review for the tourist trip design problem: extensions, solution techniques and future research lines," *Operations Research Perspectives*, vol. 9, p. 100228, 2022.
- [21] J. Zhong, X. Wang, and L. Li, "Optimization for the multiday urban personalized trip design problem with time windows and transportation mode recommendations," *Transportation Research Record*, vol. 2677, no. 5, pp. 327–340, 2023.
- [22] K. Sylejmani, V. Abdurrahmani, A. Ahmeti, and E. Gashi, "Solving the tourist trip planning problem with attraction patterns using metaheuristic techniques," *Information Technology & Tourism*, vol. 26, no. 4, pp. 633–678, 2024.

- [23] H. Sun, Y. Chen, J. Ma, Y. Wang, X. Liu, and J. Wang, "Multi-objective optimal travel route recommendation for tourists by improved ant colony optimization algorithm," *Journal of Advanced Transportation*, vol. 2022, p. 6386119, 2022.
- [24] G. Boeing, "Modeling and analyzing urban networks and amenities with OSMnx," *Geographical Analysis*, vol. 57, no. 4, pp. 567–577, 2025.
- [25] ———, "Street network models and indicators for every urban area in the world," *Geographical Analysis*, vol. 54, no. 3, pp. 519–535, 2022.
- [26] P. Taitit, K. Adhinugraha, and D. Taniar, "Navigating the maps: Euclidean vs. road network distances in spatial queries," *Algorithms*, vol. 17, no. 1, p. 29, 2024.
- [27] S. M. Nasution *et al.*, "Tourism itinerary recommendation using vehicle routing problem time windows and analytics hierarchy process," *Indonesian Journal of Electrical Engineering and Computer Science*, vol. 36, no. 1, pp. 517–534, 2024.
- [28] D. H. Fathurrohman, G. Alberto, and T. Iswari, "Application of green orienteering problem for tourism case in Yogyakarta," *Systemic Analytics*, vol. 3, no. 4, pp. 270–285, 2025.
- [29] S. Thipsingh *et al.*, "Social and sustainable determinants of the tourist satisfaction and temporal revisit intention: a case of Yogyakarta, Indonesia," *Cogent Social Sciences*, vol. 8, no. 1, p. 2068269, 2022.
- [30] D. Kaushik and M. Nadeem, "Parameter tuning in metaheuristics: a bibliometric and gap analysis," *International Journal of Information Technology*, vol. 16, pp. 1645–1651, 2024.